JOURNAL OF GEOPHYSICAL RESEARCH, VOL. 105, NO. B10, PAGES 23,727–23,740, OCTOBER 10, 2000

Experiments on conduit flow and eruption behavior of basaltic volcanic eruptions

Ralf Seyfried and Armin Freundt
GEOMAR Forschungszentrum, Kiel, Germany

Abstract: Multiphase flow in basaltic volcanic conduits is investigated using analog experiments and theoretical approaches. Depending on gas supply, large gas bubbles (gas slugs) may rise through basaltic magma in regimes of distinct fluid-dynamical behavior: ascent of single slugs, supplied slugs fed from the gas source during ascent, and periodic slug flow. An annular flow regime commences at the highest gas supply rates. A first set of experiments demonstrates that the growth of gas slugs due to hydrostatic decompression does not affect their ascent velocity and that excess pressure in the slugs remain negligible. The applicability of theoretical formulae describing slug ascent velocity as a function of liquid and conduit properties is evaluated in a second set of experiments. A third set of experiments with continuous gas supply into a cylindrical conduit are scaled to basaltic conditions over Morton, Eotvös, Reynolds, and Froude numbers. Gas flow rate and liquid viscosity are varied over the whole range of flow regimes to observe flow dynamics and to measure gas and liquid eruption rates. Foam generation by slug bursting at the surface and partial slug disruption by wake turbulence can modify the bubble content and size distribution of the magma. At the transition from slug to annular flow, when the liquid bridges between the gas slugs disappear, pressure at the conduit entrance drops by ~ 60% from the hydrostatic value to the dynamic -flow resistance of the annular flow, which may trigger further degassing in a stored magma to maintain the annular flow regime until the gas supply is exhausted and the eruption ends abruptly. Magma discharge may also terminate when magma ascent is hindered by wall friction in long volcanic conduits and the annular gas flow erodes all magma from the conduit. Supplied slugs are found to reach much higher rise velocities than unsupplied slugs and to collapse to turbulent annular flow upon bursting at the surface. A fourth set of experiments uses a conduit partially blocked by built-in obstacles providing traps for gas pockets. Once gas pockets are filled, rising gas slugs deform but remain intact as they move around obstacles without coalescence or significant velocity changes. Bursting of bubbles coalescing with trapped gas pockets causes pressure signals at least 3 orders of magnitude more powerful than gas pocket oscillation induced by passing liquid. Our experiments suggest a refined classification of Strombolian and Hawaiian eruptions according to time-dependant behavior into sporadically pulsating lava fountains (driven by stochastic rise of single slugs), periodically pulsating lava fountains (resulting from slug flow), and quasi-steady lava fountains (oscillating at the frequency of annular-flow turbulence).

1. Introduction

Through the past decade, there has been a strong research focus on Plinian eruptions of felsic, highly viscous magmas involving physical and experimental modeling of the dynamics of degassing, magma fragmentation, and eruption column ascent. Magma fragmentation in such eruptions has been ascribed to bubble overpressure, high elongation rates or high shear rates associated with the enormous acceleration driven by gas expansion [e.g., *Sparks*, 1978; *Proussevitch et al.*, 1993a; *Sugioka and Bursik*, 1995; *Zhang et al.*, 1997; *Alibidirov and Dingwell*, 1996; *Mader et al.*, 1994; *Gardner et al.*, 1996; *Papale*, 1999]. However, ~70% of the bulk annual subaerial magma discharge to the Earth's surface is produced by basaltic volcanic eruptions, which occur continuously all around the Earth [*Simkin and Siebert*, 1994] and are characterized by longtime activity but produce low fountains and ash clouds limited to the troposphere. The eruption dynamics of basaltic magmas, which have a much lower viscosity and lower gas contents than felsic magmas, have found little attention since *Wilson and Head* [1981] physically described Hawaiian-style eruptions evolving from homogeneous degassing of magma assumed to fragment upon reaching a critical threshold vesicularity (70-80%). Fragmentation models derived for highly viscous felsic magma cannot simply be applied to low-viscosity basaltic magma because comparably high shear rates cannot be supported and gas bubbles are free to move and expand.

Wilson and Head [1981] and *Parfitt and Wilson* [1995] consider homogeneous gas-magma flow in the conduit, i.e., gas bubbles moving with the magma while they expand during ascent to the surface. *Wilson and Head* [1988] did, however, also draw attention to the possibility of bubble coalescence and the occurrence of separated gas-magma flow, in which bubbles move relative to each other and to the magma. *Vergniolle and Jaupart* [1986], *Jaupart and Vergniolle* [1989], and *Vergniolle and Jaupart* [1990] demonstrated by experiment and theory that a trapped foam layer can form under the roof of a reservoir by volatile exsolution from the stored magma, even

Paper number 2000JB900096.
0148-0227/00/2000JB900096$09.00

if a conduit already exists. When exceeding some critical depth, the foam layer collapses and releases a large volume of gas into the conduit, generating separated gas-magma conduit flow.

The distinction between homogenous and separated gas-magma flow is important when considering the gas mass eruption rate, which is directly coupled with the initial dissolved magmatic volatile content in the case of homogeneous flow but is decoupled from volatile content in separated two-phase flow. This paper investigates basaltic magma eruption dynamics based on separated two-phase flow using the investigations of Vergniolle and Jaupart as a starting point. However, the present study focusses on the dynamics of separated two-phase flow in the conduit, rather than on its generation. The experiments of Vergniolle and Jaupart were not scaled to volcanic conditions, liquid viscosity was not varied, and slug ascent (slug = large gas bubble almost filling the conduit diameter) was assumed to occur only in the inertial regime of single slug ascent where it does not depend on magma rheology. We will show in the following that separated two-phase flow may proceed in different regimes: single-slug ascent occurs from the sporadic release of limited gas volumes into the conduit; supplied slugs remain connected to, and fed from, a gas source over the whole time of their ascent through the conduit; slug flow, i.e., a periodic sequence of ascending gas slugs, arises from continuous gas release at moderate rates; and turbulent annular flow, in which a central gas stream erodes and mixes with marginal liquid, forms from gas release at high rates.

These regimes of separated two-phase conduit flow involve distinct formation conditions and ascent dynamics, which differ from the theory of *Vergniolle and Jaupart* [1990]. We use four different experimental simulations complemented by theoretical considerations to investigate the role of these different two-phase flow regimes in basaltic eruptions.

2. Ascent of Single Gas Slugs

2.1. Theoretical Framework

Three dimensionless fluid-dynamical parameters are necessary to derive the terminal ascent velocity U_{sl} of buoyantly rising single gas slugs: Froude number,

$$Fr = \frac{w^2}{gD}, \tag{1}$$

which represents the ratio of kinetic to potential energy, Eotvös number,

$$Eo = \frac{\rho g D^2}{\sigma} \tag{2}$$

which evaluates gravity force against surface force, and Morton number,

$$Mo = \frac{g\mu^4}{\rho\sigma^3}, \tag{3}$$

which relates viscous to surface forces, with g the gravitational acceleration, ρ the liquid density, μ the liquid

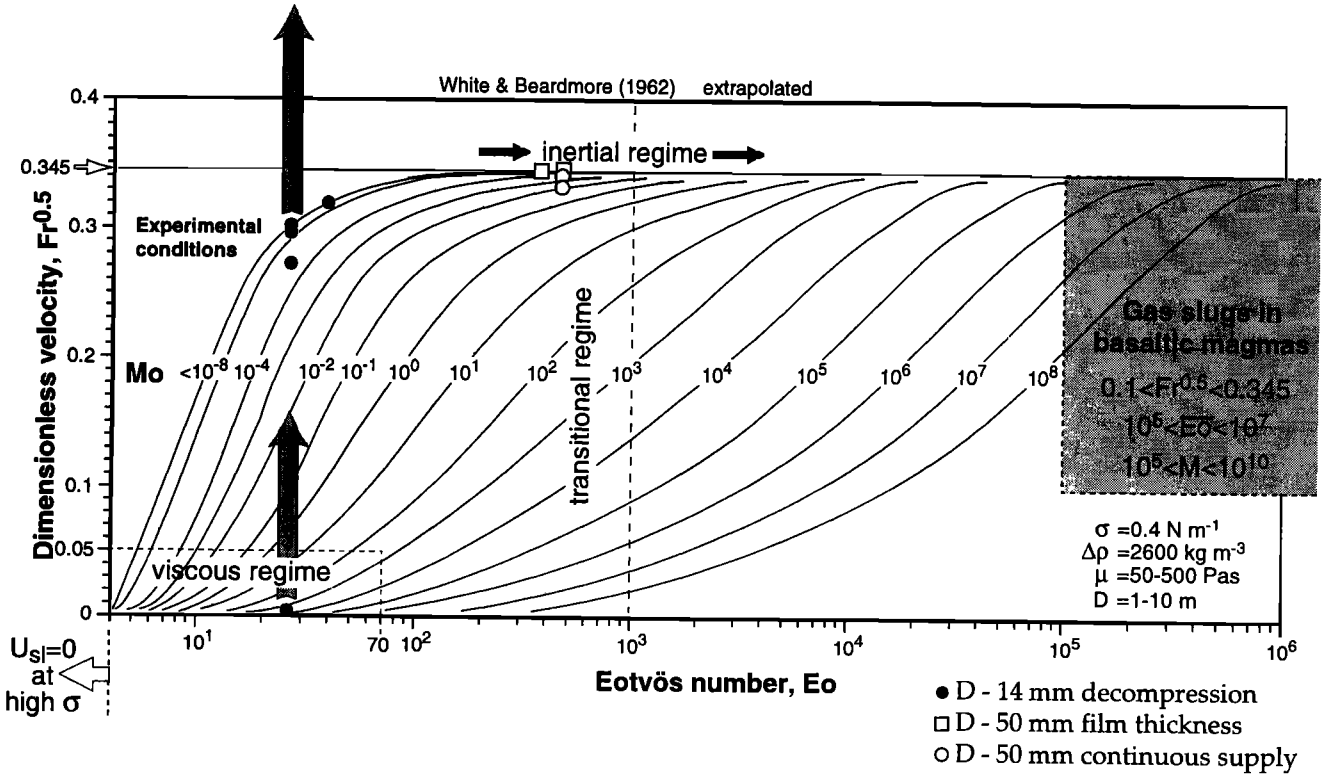

Figure 1. *White and Beardmore* 's [1962] diagram for slug ascent velocities in dimensionless writing, extrapolated to volcanic conditions. The square root of the Froude number represents the dimensionless ascent velocity. Eotvös number can be interpreted as dimensionless conduit diameter. Morton numbers represent different liquid rheologies. Symbols give experimental data for unsupplied slugs; arrows point to corresponding velocities of supplied slugs under otherwise constant conditions. Shaded field on the right outlines parameter ranges for gas slugs in basaltic magma, extending from the inertial through the transitional regime.

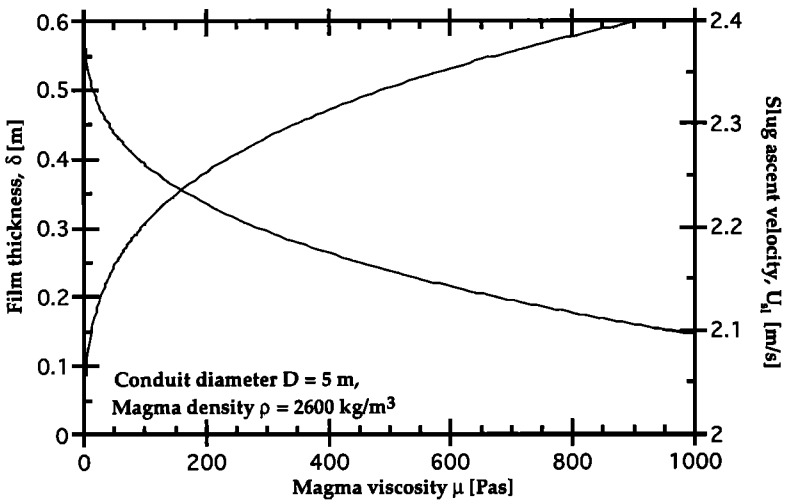

Figure 2. Film thickness δ (left axis) from (6) and slug ascent velocity U_{sl} (right axis) from (7) versus magma viscosity μ for a basaltic conduit diameter of D = 5 m and magma density ρ = 2600 kg/m^3.

viscosity, and σ the surface tension. Inertial forces dominate at Mo < 10^{-6} and Eo > 100, viscosity and surface tension influences become negligible, and the ascent velocity of gas slugs reaches the highest value, depending on conduit diameter D only [*White and Beardmore,* 1962] as

$$U_{sl}(i) = 0.345\sqrt{gD}. \quad (4)$$

No separated slug rise ($U_{sl} = 0$) occurs for Eo < 3.4, where surface tension is dominant [*Wallis*, 1969].

The inertial velocity $U_{sl}(i)$ from (4) is commonly assumed in two-phase flow modeling of basaltic eruptions [e.g., *Vergniolle and Jaupart*, 1990]. However, for a typical rheology of basaltic magma

σ=0.4 N/m; ρ=2600 kg/m^3; μ=500 Pas; 1<D<10 m

we obtain

$$0.1 < Fr^{0.5} < 0.345;\ 10^5 < Eo\ 10^7;\ 10^5 < Mo < 10^{10}$$

suggesting that slug ascent in basaltic magma lies in the transitional regime where $U_{sl} < U_{sl}(i)$. In the transitional regime, U_{sl} should depend on slug length and magma viscosity. Figure 1 shows slug ascent velocities in dimensionless form after *White and Beardmore* [1962]; we extrapolated this diagram to include volcanic properties.

The ascent rate of a slug is controlled by the volume flux of liquid from the bubble head to its wake. Hence, a thin liquid counter-flow film wraps the slug. The equilibrium between buoyancy, viscous, and surface forces controls the shape and rate of the film flow. The elongated bubble can be divided into a convex cap region and the cylindrical body, along which film thickness $\delta=0.5(D-d_{sl})$ is constant; D and d_{sl} are the conduit and slug bubble diameters, respectively. *Brown* [1965] related film thickness to ascent velocity through the parameter

$$N = \sqrt{14.5\frac{\rho^2 g}{\mu^2}}, \quad (5)$$

which evaluates buoyancy against viscous forces, leading to an expression that yields δ from rheological parameters and conduit geometry as

$$\delta = \sqrt{\frac{1+ND-1}{N}}. \quad (6)$$

Figure 2 shows film thickness δ as a function of liquid viscosity using (6). Slug ascent velocity and film thickness are related as [*Brown*, 1965]

$$u = 0.345\sqrt{g(D-2\delta)}. \quad (7)$$

The variation of slug velocity with magma viscosity after equation (7) is also shown in Figure 2. Application of (7) is limited to

$$Eo = \left(1-\frac{2\delta^2}{D}\right) > 5.0$$

for the surface tension, and to ND > 60 for the viscosity.

2.2. Slug Expansion

Equations (5) – (7) having been derived for engineering applications, assume constant slug length during ascent through an infinite conduit. In long volcanic conduits, however, rising gas slugs will increase in length, L_{sl}, due to decompression of the gas. Gas density ρ_g decreases with depth z as hydrostatic pressure diminishes and is given by

$$\rho_g(z) = \frac{\rho g z + P_a}{RT}, \quad (8)$$

neglecting excess pressure effects, where ρ is magma density, R is gas constant, T is temperature, P_a is atmospheric pressure. Gas slug volume and length at depth z then are

$$L_{sl} = \frac{1}{A}V_{sl} = \frac{m_g RT}{\rho g z + P_a} \quad (9)$$

with m_g is gas mass and A is slug cross-sectional area. The increase in volume with decreasing z is

$$\frac{V_{sl}}{dz} = -\frac{m_g RT\rho g}{(\rho g z + P_a)^2} = A\frac{L_{sl}}{dz}. \quad (10)$$

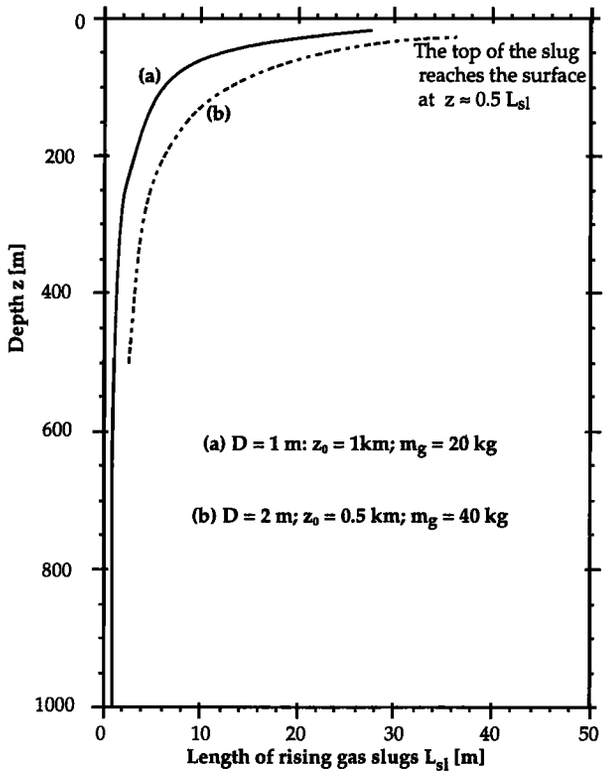

Figure 3. Increase in slug length due to decompression during approach to the surface from (9) for two sets of initial values of conduit diameter D, depth of slug origin z_0, and gas mass m_g contained in the slug.

Figure 3 shows that the length of gas slugs rising through a volcanic conduit can increase by more than an order of magnitude from expansion alone and will further increase if volatiles such as H_2O continue to exsolve during approach to the surface. Gas slug pressure P_{sl} is the sum of hydrostatic pressure and excess pressure terms due to inertial, viscous, and surface tension resistance to slug expansion [*Sparks*, 1978; *Proussevitch et al.*, 1993b]:

$$P_{sl}(z) = P_a + \rho g z + \rho_m U_{sl}^2 \left[\frac{dL_{sl}}{dz}\frac{d^2L_{sl}}{dz^2} + 1.5\left(\frac{dL_{sl}}{dz}\right)^2 \right] + \frac{dL_{sl}}{dz}\frac{4\mu U_{sl}}{L_{sl}} + \frac{2\sigma}{L_{sl}} \quad (11)$$

hydrostatic + inertial forces + viscous + surface forces.

However, for basaltic magma rheology and relevant values of U_{sl} and L_{sl} ($\mu > 50$ Pas, and D, $L > 2$ m) the excess pressure terms remain negligible.

If, for example, we assume D = 2 m, μ = 100 Pa s, ρ = 2600 kgm^{-3}, m_g = 1 kg, R = 461 Jkg^{-1}K^{-1}, z = 1 m, , T = 1400 K, U_{sl} = 1.5 m/s, σ = 0.4 kgm^{-1}, we obtain L_{sl} = 1.6 m from (9) and dL_{sl}/dz = -0.33 from (10). Since

$$\frac{d^2L_{sl}}{dz^2} = \frac{4\rho^2 g^2}{A}\frac{m_g RT}{(\rho g z + P_a)^3}, \quad (12)$$

$d^2L_{sl}/dz^2 = 10^{-5}$, so that we obtain the terms in (11) as

Psl(z) = 125,500+956+375+0.5 Pa

where the first (hydrostatic) term exceeds the other terms by more than 2 magnitudes. This example calculation is conservative since increasing z will decrease dL/dz and d^2L/dz^2 but increase the hydrostatic pressure term. Thus, slug-length increase will follow the hydrostatic decompression during ascent without development of significant overpressure in the bubble.

2.3. Decompression Experiments

Our first set of experiments was designed to investigate the effect of decompressional length growth on slug ascent velocity. We measured length and velocity from video recordings following the ascent of gas slugs along a 4-m long vertical perspex tube of 14 mm diameter (Figure 4). A fixed-volume steel tube filled with gas at a controlled pressure allowed injection of a pre-defined mass of gas into the perspex tube, which was filled with one of the following four liquids:

1. Pure water
μ = 1 mPa s; ρ = 1000 kgm^{-3}; Mo = 2.8x10^{-11}; Eo = 27.5

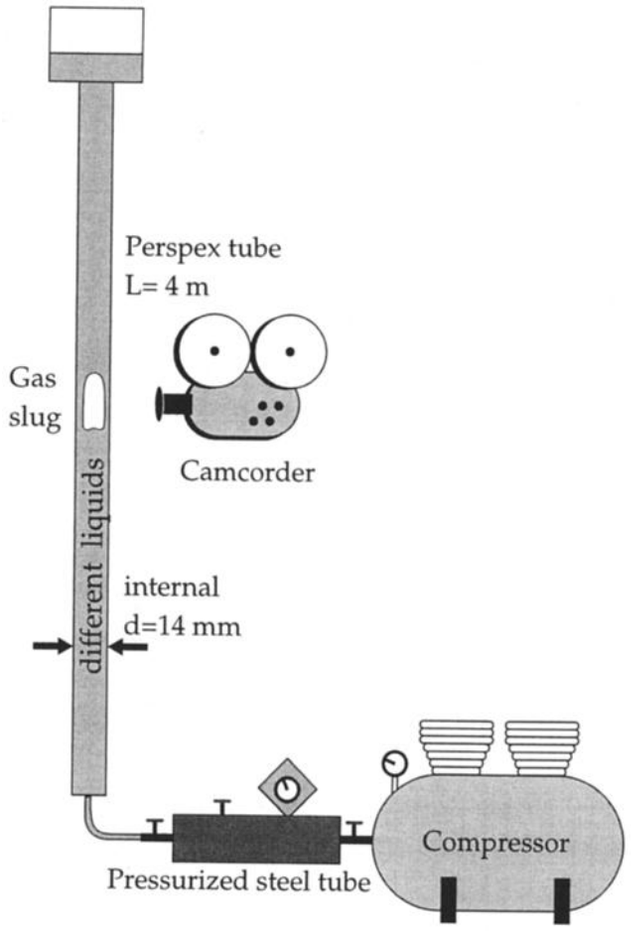

Figure 4. Experimental setup to measure ascent velocity and decompressional length increase of gas slugs. Air is enclosed under a defined pressure in a steel tube in order to release slug bubbles of a defined gas mass into the conduit.

2. Water-sodium-polywolframate solution
μ = 1 mPa s; ρ = 1400 kgm^{-3}; Mo = 4x10^{-11}; Eo = 38.5

3. Water-cellulose ester solutions
a) μ = 13 mPa s; ρ = 1000 kgm^{-3}; Mo = 8x10^{-7}; Eo = 27.5
b) μ = 22 mPa s; ρ = 1000 kgm^{-3}; Mo = 1x10^{-5}; Eo = 27.5

The hydrostatic pressure drop along the tube was 3.9x10^4 Pa, (5.5 x 10^4 Pa for liquid 2). The small tube diameter implies a very low value of Eo so that the experiment is not properly scaled to a volcanic conduit, but it is sufficient for the comparison of slug ascent rates under decompression to those derived from theoretical predictions given above. Slug ascent behavior in volcanic conduits, where the Eotvös number is much higher, will also be influenced by rough walls and non circular cross section of the conduit, and by the scavenging of volatiles from the magma and of small bubbles from the conduit wall region into the slug. However, such phenomena are treated separately in section 5.

With all four liquids, the ascent velocity of decompressing gas slugs remained constant during passage through the 4 m long tube although slug lengths increased by up to a factor 1.4. This observation is attributed to the balance between increasing buoyancy (driving force) and increasing slug surface (resistance force). Ascent velocity did, however, increase weakly with the initial gas mass forced into the conduit (Figure 5). Slugs with a higher gas mass are longer than those with a lower gas mass at any pressure level. Ascent velocity increases weakly with slug length at a defined pressure but it does not change with increasing length of a slug of constant gas mass. Considering the limited overall range of slug velocities, however, deviations in velocity of < 7% appear to be negligible so that the experimental results match well with the predictions of (6) and (7).

2.4. Analysis of the Counter Flow Film

A second set of experiments is used to analyze liquid film thickness and slug cap geometry. To study the counter flow behavior around a slug, it was necessary to use a larger tube diameter. We measured the liquid film thickness of slugs in a square perspex tube of width l = 50 mm, using transmitted light with a schlieren system. A square tube avoids the optical distortion of a cylindrical tube, although the results cannot be directly compared due to the stronger liquid backflow in the tube corners. We performed our calculations using the corresponding tube diameter

$$D' = \sqrt{\frac{4}{\pi}}l = 0.0564 \text{ m} \qquad (13)$$

and we obtain Eo = 455 for all liquids used, and

Mo = 2.86X10^{-11}	for 1 mPa s,
Mo = 6 X 10^{-7}	for 12 mPa s,
Mo = 1.45X 10^{-2}	for 150 mPa s.

Measurements in a circular conduit D = 50 mm filled with pure water were made for comparison at Eo = 350 and Mo = 2.86X10^{-11}.

The experimental conditions are in the inertial regime $Fr^{0.5}$ = 0.345 except for the highest-viscosity runs (Figure 1), which lie in the transitional regime where a significant film thickness may be expected, as shown in Figure 6. Film thickness approaches a value unmeasurably small at the bottom of the cap in the lower-viscosity liquids (1 and 12 mPa s) and approaches a constant value of 3 mm in the high-viscosity liquid (150 mPa s). Film thickness is slightly overestimated by (6) with respect to measured data (Figure 6), which will be due to increased back flow in the corners of the square conduit. In contrast to theoretical

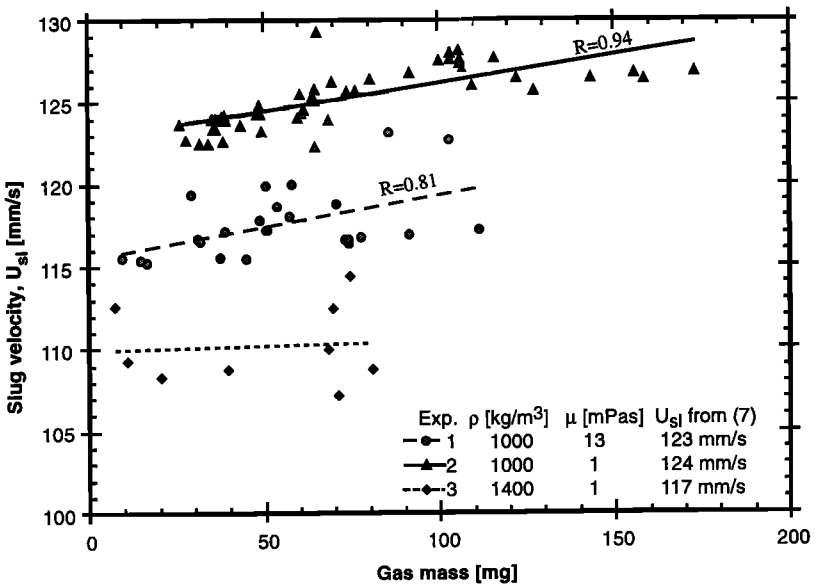

Figure 5. Ascent velocities of decompressing gas slugs, measured in the setup of Figure 4, versus their contained gas mass. Symbols distinguish three sets of data for three liquids (1 to 3) of different values of ρ and μ as tabulated. Lines labelled E are linear regressions through experimental data; no reasonable regression was possible for data set 3 due to wide scatter. Regression residuals R for sets 1 and 2 are indicated. Horizontal lines labelled T indicate corresponding theoretical velocities calculated from (7) which are independent of gas mass. Measured data scatter around theoretical values but show a weak increase in velocity with gas mass.

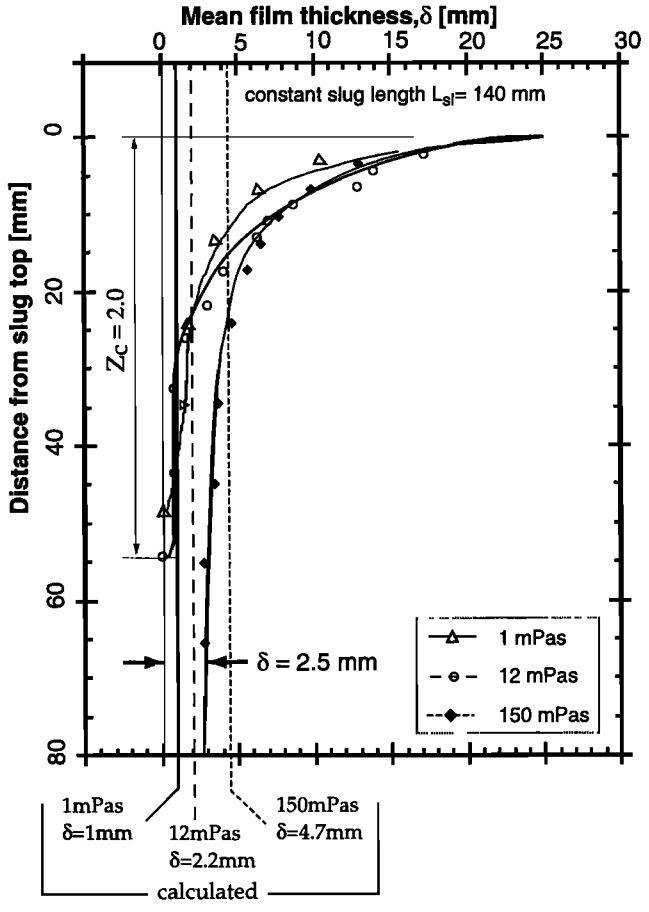

Figure 6. Measured decrease in film thickness δ with distance below slug top for three liquid viscosities in a 50-mm-wide tube. Film thickness approaches a constant value below z_C, the height of the slug cap. Vertical lines indicate δ values for each viscosity after (6) for comparison.

predictions, the experimental measurements show that film thickness decreases with slug length at constant liquid viscosity (e.g., μ = 150 mPa s in Figure 6). Figure 7 illustrates the change in slug shape with length. Measured slug velocities in the inertial regime (low-viscosity liquids) correspond closely to theoretically expected values, but we note that published theoretical approaches [e.g. *Clift*, 1978; *Wallis*, 1969] do not address the complex relationships of slug ascent in the transitional regime.

Further complications arise from the rising behavior of gas slugs. Turbulent liquid backflow disrupts the bottom of a slug in the inertial regime and creates a swarm of small bubbles in its wake. *Campos and Guedes de Carvalho* [1988] found that an axis-symmetric laminar wake prevails at Re < 180, and wake vortex rings start to oscillate at 180 < Re < 300, and become fully turbulent at Re > 300. We may assume approximate Hawaiian conditions as a volcanic example (D = 10 m; μ = 50 Pa s; ρ = 2600 kgm^{-3}) and obtain U_{sl} = 3.4 ms^{-1} (equation (4)) and Re = 1768, suggesting fully turbulent conditions under which slug disruption and introduction of small bubbles into the magma may occur as observed in the experiments. In the transitional regime (higher-viscosity liquid) a bubbly wake did not form in our experiments. Instead, the liquid backflow was laminar with a visible film thickness, the slug cap length was longer, and the film thickness decreased with increasing slug length. However, the collapse of each slug at the conduit exit mixed small bubbles into the liquid which were slowly carried down into the conduit by the back flow of liquid so that a foam film formed around slugs as the two-phase conduit flow proceeded (Figure 8). With a foamy liquid film, counter flow is weaker so that slug ascent velocity is reduced.

The admixing of bubbles to the liquid may have some implications in basaltic volcanic eruptions. Small bubbles introduced into the liquid either by turbulent slug wakes or by slug collapse at the surface and liquid back flow may affect bubble size distributions in the liquid as it is frozen in. The thermal insulation of the conduit is improved by bubbly marginal magma. At low strain rates the presence of additional bubbles increases the effective magma viscosity [e.g. *Vergniolle and Jaupart*, 1990], thus reducing slug ascent velocities (equations (4)-(7)). At high strain rates (high Capillary numbers), disruption of bubbles along the conduit walls has been proposed to cause lubrication and acceleration of the central conduit flow [*Stein and Spera*, 1992; *Herd and Pinkerton*, 1997]. However, with slug flow velocities in the range 1-5 ms^{-1} as deduced here, strain rates will be too low to deform the bubbles as can be seen on Figure 8.

2.5. Supplied Slugs

We define a supplied slug as a large gas bubble that remains connected to, and fed from, its source gas reservoir during passage through the conduit. No backflow occurs and the ascent velocity is controlled by the rate of gas influx so that we would expect it to be higher than the ascent velocity of unsupplied slugs (equations (4) and (7)). Indeed, supplied slugs reached $Fr^{0.5}$ = 1.3 (Figure 1) in an experimental tube of 50 mm diameter filled with pure water (1 mPa s), where the equilibrium ascent velocity of an unsupplied slug would lie on the limiting asymptote $Fr^{0.5}$ = 0.345. Repeating this experiment with a thinner tube of 14 mm diameter and more viscous liquid (5000 mPa s), supplied slugs reached $Fr^{0.5}$ = 0.16 (Figure 1) compared to unsupplied slugs which would hardly move at $Fr^{0.5}$ = 0.01. Supplied slugs thus reach 10 times the limiting equilibrium velocity value of unsupplied slugs (Figure 1). The column of dense liquid above a supplied slug is pushed out of the conduit until the slug cap reaches the surface. When the slug cap bursts at the surface, the slug breaks down into a turbulent two-phase flow and a quasi-steady fountain of liquid spray is ejected from the conduit. This behavior was observed in both low- and high-viscosity liquid experiments.

Supplied slugs in the experiments formed only when the valve at conduit bottom controlling gas influx was opened suddenly, that is when the acceleration of the injected gas mass flow (dM_g/dt) was high, and when the injected bulk gas volume was larger than the conduit volume. Slow opening of the valve resulting in low values of dM_g/dt, i.e., gradual acceleration of the gas mass flux, resulted in the evolution of separated two-phase flow regimes discussed in section 3. The occurrence of supplied slugs in basaltic volcanoes thus requires the sudden release of a large gas volume, such as in the case of a catastrophically collapsing foam layer as envisioned by *Jaupart and Vergniolle* [1989].

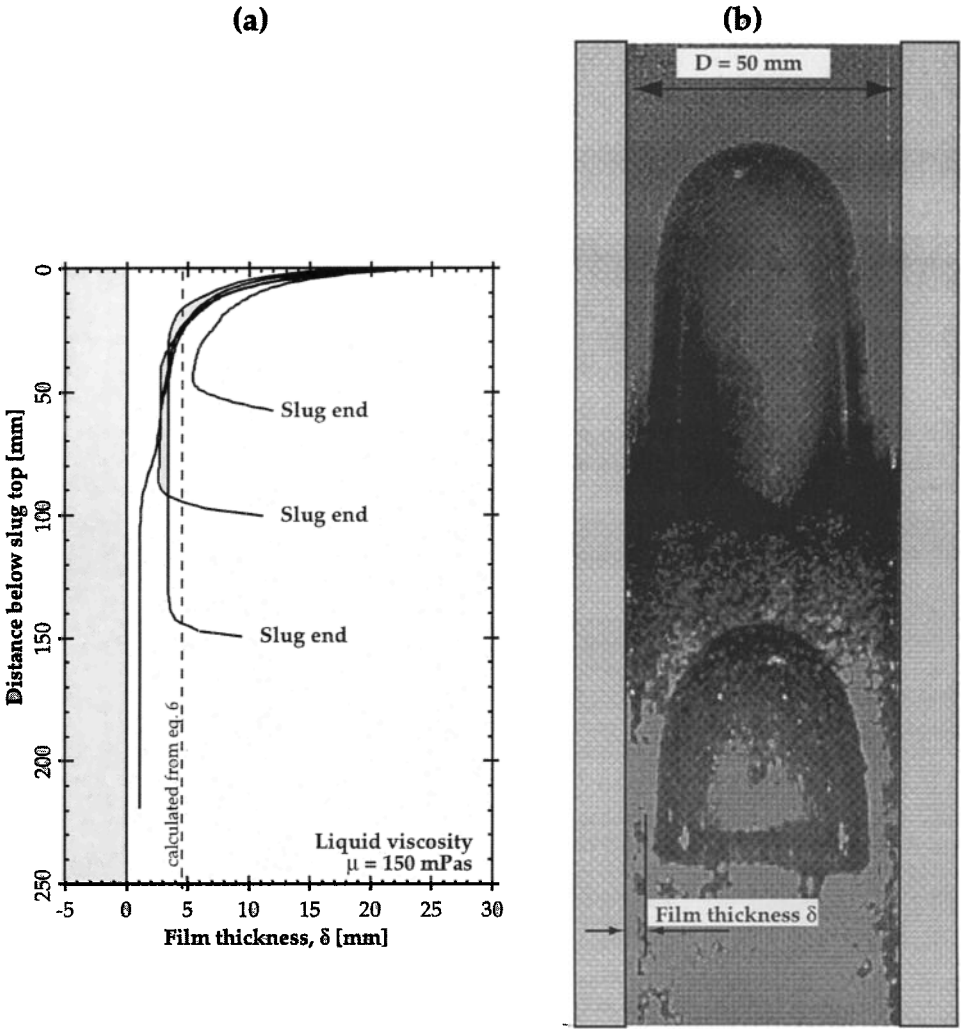

Figure 7. (a) Film thickness versus depth below slug top as in Figure 6 but for slugs of different lengths in liquid of constant viscosity. Asymptotic film thickness decreases toward longer slugs. Vertical dashed line shows δ value from (7) for comparison. (b) Schlieren picture of two slugs of different lengths in the 50-mm conduit. Note train of small bubbles in the wake of the upper slug.

3. Continuos Gas Supply

3.1. Theory of Slug flow and annular flow

A continuous gas stream injected into a liquid column is known to be unstable and transforms into various types of separated two-phase flow [*Wallis*, 1969]. In the slug flow regime a continuous gas stream breaks up into a chain of equally spaced slug bubbles of ascent velocity U_{sf}, which is greater than the velocity of corresponding isolated slugs, U_{sl}, by the mean gas volume flux Q_g [*Wallis*, 1969] such that

$$U_{sf} = \frac{Q_g}{A} + U_{sl}\ , \tag{14}$$

The mean velocity of the bulk mixture across the cross sectional area of the conduit, A, is constant from continuity,

$$J = \frac{Q_g + Q_l}{A}\ . \tag{15}$$

Here, Q_l is the net upward flux of liquid which reflects the difference between the upward transported liquid between gas slugs and the liquid flowing downward through the marginal film region wrapping the slugs. In contrast to single-slug ascent, where film liquid just circulates around the bubble, in the slug-flow regime there is an effective transport of film liquid downward in the conduit as observed in our experiments. The downward flux of liquid depends on liquid viscosity through the film thickness δ.

Slug flow transforms into annular flow when the liquid bridges between the gas slugs disappear with increasing gas influx. Coalescence of gas slugs then is facilitated by increasing turbulence in the liquid bridges. *Wallis* [1969] reports a criterion for the transition from slug to annular flow that depends on the flux of liquid Q_l:

$$\frac{Q_g}{AU_{sf}} = 0.4 + 0.6\frac{Q_l}{AU_{sf}}. \tag{16}$$

3.2. Experiments With Continuous Gas Supply

Having investigated the ascent of slugs introduced singly into the conduit, we now address the two-phase flow dynamics that result from a continuous gas supply. This third set of

Figure 8. Photograph of bubbly liquid back flow partly obscuring the rising gas slug in the center of the pipe. Width of picture is 50 mm.

experiments was designed to measure the mass balance of liquid and gas ejected from the conduit and to determine the pressure changes within, and at the transitions between, different flow regimes. These experiments were scaled to natural basaltic volcanic conditions.

3.2.1. Scaling of the experiments. Under volcanic conditions, gravity forces surmount surface forces by orders of magnitude if we consider the scale of the conduit flow profile rather than the behavior of individual bubbles. Our choice of experimental Eotvös numbers Eo = 335 ascertains that gravity forces surmount surface forces by more than 2 magnitudes. Eotvös numbers for volcanic conduits would be higher at Eo > 10^5, but higher Eo values have no effect on the flow behavior as long as the critical value for gravity-dominance is exceeded.

Scaling in the annular flow regime uses the two-phase flow Reynolds number,

$$Re_{2p} = \frac{JD\rho_{an}}{\mu}, \quad (17)$$

which must be $Re_{2p} > 2300$ to maintain turbulent conditions, and the two-phase flow number, N_{2p}, introduced by *Wallis* [1969], which provides a lower limit $N_{2p} > 100$ to annular flow formation. In the annular flow regime, the central flow is a particle-laden gas jet of viscosity $\mu_{an} = 10^{-4}$ Pa s [*Kieffer*, 1977] that erupts gas and liquid at a mass ratio

$$k_m = \frac{M_l}{M_g}, \quad (18)$$

where M_g and M_l are the measured erupted mass fluxes of the two phases. The density of the mixture, ρ_{an} can be obtained from

$$\rho_{an} = \frac{\rho_g + k_m\rho_l}{1+k_m}. \quad (19)$$

For typical experimental values of M_l = 25 g/s and M_g = 0.5 g/s (k_m = 50), we obtain Re_{2p} = 4000, that is higher than the minimum value required for turbulent flow. The two-phase flow number satisfied $N_{2p} > 100$ for experimental liquid viscosities < 400 mPa s. However, we did not observe significant changes in flow behavior at viscosities > 400 mPa s and therefore we also include results for higher viscosity values in our discussion. For volcanic conditions (assuming μ = 100 Pa s, ρ_l = 2600 kgm^{-3}, D = 5 m, and k_m = 50), Re_{2p} varies with depth in the conduit but $Re_{2p} > 2300$ if $J > 18$ ms^{-1} is a condition easily satisfied at least at upper conduit levels. Using the same μ and ρ_l values, the volcanic two-phase flow number is $N_{2p} > 100$ if D > 1 m (e.g., N_{2p} = 910 for D = 5 m). Again, no significant changes in flow regime occur with further increase of either Re_{2p} or N_{2p} as long as the limiting values for a given flow regime are satisfied. The same holds for the Morton number (equation (3)), which is much higher in the volcanic than in the experimental system (Figure 1), but the dominance of viscous over surface forces is maintained in both systems.

3.2.2. Experimental setup. The experimental setup (Figure 9) consists of a liquid-filled perspex tube of 1 m length with 50-mm-wide square cross section connected to a liquid reservoir of 100 L. Compressed air is injected via four nozzles at the base of the conduit to establish two phase flow over the whole length of the conduit. Liquid exhausted from the top of the tube was sampled in a container divided into concentric ring-segments, which allowed us to determine radial liquid mass distribution from experimental eruptions. In most experiments, however, erupted liquid was allowed to flow back into the large reservoir in order to maintain steady-state conditions. Bubbly flow, slug flow, and annular flow could be produced in the conduit without significant changes in liquid level and hydrostatic pressure. Flow behavior, bubble sizes, and velocities were determined from video recordings. Liquid viscosity was varied logarithmically from 1 to 1200 mPa s by dissolving cellulose ester in water. Basal pressure in the conduit was measured 100 mm above the gas injection level. Gas volume flow was measured before the injection and could be converted into mass flow using measured temperature and pressure data. An inductive, viscosity-independent liquid mass flow meter was placed between reservoir and conduit. In these experiments the gas-inlet valve was opened slowly (low dM_g/dt) to avoid formation of supplied slugs.

3.2.3. Liquid-friction effects. Liquid mass flux from the conduit was controlled by the two-phase flow dynamics at low liquid viscosities, but friction in the liquid plumbing system limited the flux at high viscosities. Most of liquid friction occurred in the narrow cross section of the flow meter (D_{in}=10 mm). Conditions of Re < 600 within the pipe allow the friction coefficient λ to be determined from the Hagen-Poiseuille law,

$$\lambda = 64/Re. \quad (20)$$

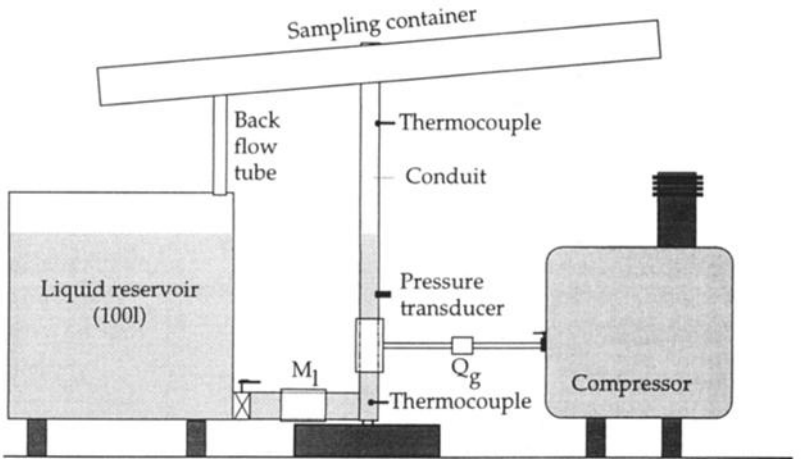

Figure 9. Setup for experiments with continuous gas supply consisting of a liquid-filled perspex tube of 1 m length with square cross section of 50 mm connected to a liquid reservoir of 100 L. Exhausted liquid was sampled in a container, and could flow back into the liquid reservoir to provide constant flow conditions for long time measurement. Mass flux of liquid M_l, and volume flux of gas Q_g, were measured at the respective entries.

For constant liquid density and pipe geometry, λ increases with viscosity and is indirectly proportional to the mass flow. Hence, an asymptote forms as M_l tends to zero so that

$$\lambda = 16\pi D_{in}\frac{\mu}{M_l}, \tag{21}$$

and the pressure loss Δp along the length L_{in} of the inlet pipe,

$$\Delta p = 128\mu\frac{M_l L_{in}}{\rho\pi D_{in}^4}. \tag{22}$$

The pressure loss (Δp) increases from only 40 Pa for the lowest viscosity of $\_ = 1$ mPa s and $M_l = 50$ gs^{-1} up to 10^4 Pa for $\_ = 1200$ mPa s and $M_l = 10$ gs^{-1}.

When the pressure loss approaches the hydrostatic pressure value of 7000 Pa in the reservoir, the rate of liquid supply can no longer balance the rate of liquid ejection by the two-phase flow and the conduit is emptied of liquid as the experiment proceeds.

3.2.4. Experimental results. A steady gas supply injected into a liquid column may break up into an unsteady, pulsating flow in the conduit depending on the gas flow rate [*Wallis*, 1969]. With increasing gas supply we observed gradual changes in flow regime in our experiments, from bubbly flow through slug flow to annular flow for higher viscosities. The transitions in flow regime shifted to lower gas supply rates at higher liquid viscosities. In the slug flow regime the length of each bubble increased with the rate of gas supply but decreased with increasing liquid viscosity. Quantitative results varied with the way gas was introduced into the conduit and with the duration of the experiments. Experiments could be run only for a limited time before the effects of longtime mixing, making the liquid foamy (see section 2.4, Figure 8), began to disturb the flow pattern.

In a series 1 of experiments, gas supply was kept constant for at least 20 s after unsteady injection to measure stationary flow conditions. Experiments were terminated before liquid mixed with gas bubbles. Data collected at a sampling rate of 10 Hz provided ~ 200 data points for each parameter.

In a series (2) of experiments, gas supply was slowly increased from 0.5 gs^{-1} (where first exhaustion of liquid from the conduit was observed) up to 2 gs^{-1} (where annular flow commenced). Liquid was allowed to mix with bubbles in these longer-lasting runs, and data were recorded at 20 Hz.

For both series, electronically recorded data were used to

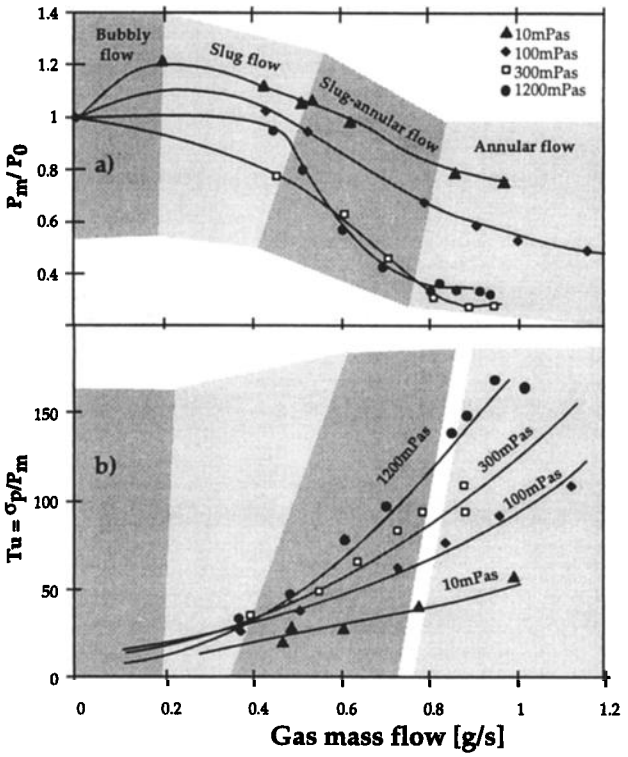

Figure 10. Results of series 1 experiments with continuous gas supply, terminated before significant mixing of bubbles into liquid occurred. Variation of (a) normalized pressure p_m/p_0, (b) measure of turbulence Tu, and (c) mass ratio k_m with gas flux. No liquid could be exhausted over the top of the conduit and $k_m = 0$ at gas mass flow rates <0.5 gs^{-1}. Note how flow regime boundaries shift with respect to the gas flux scale as liquid viscosity increases. Lines are visual fits to the data. Vertical dashed line indicates *Wallis'* [1969] criterion (equation (17)) for the slug flow to annular flow transition.

evaluate mean pressure p_m, mean gas mass flow M_g, and mean liquid mass flow M_l. The relation between standard deviation, σ_p, and mean pressure, p_m is used as a measure of the turbulence as

$$Tu = \frac{\sigma_p}{p_m} 100\ [\%]. \quad (23)$$

Results from series 1 pressure measurements are shown in Figure 10a. Pressure p_m is normalized to hydrostatic pressure (p_0) in the liquid column before onset of the experiment in order to eliminate pressure changes arising from small length changes of the liquid column due to ejection of liquid: p_m increases during the change from bubbly to slug flow in low-viscosity liquids ($\mu < 100$ mPas) due to the elevation of the liquid column by the volume of the gas phase. In the slug flow regime, p_m did not change significantly, but a rapid decrease in pressure occurred as turbulence increased with approach to slug-annular flow. The transitional region between slug and slug-annular flow narrows with increasing liquid viscosity, which is best seen by the rapid pressure decrease at a gas flux of 0.5 gs^{-1} for the highest-viscosity liquid (1200 mPa s; Figure 10a). *Wallis'* [1969] criterion, equation (16), for the transition from slug to annular flow is independent of viscosity and lies at 0.55 gs^{-1} for the given conditions.

Two-phase turbulence increases continuously with increasing gas supply rate and liquid viscosity (Figure 10b), and pressure becomes controlled by the dynamic force of the turbulent two-phase flow, rather than by the hydrostatic pressure gradient, when the liquid bridges between the slugs disappear during transition from slug to annular flow. As liquid flow resistance increases with viscosity, the pressure drop forcing the flow upward also increases, resulting in an increase in Tu (equation (23)) that promotes mixing of small bubbles into the liquid.

The mass ratio k_m of erupted liquid to gas tends to zero at very low gas supply rates (Figure 10c) as the gas flow cannot eject liquid from the conduit. A maximum in k_m is reached at the transition from slug to annular flow, followed by a decrease in k_m toward annular flow due to increased friction (equation (19)) limiting the liquid supply so that it cannot balance liquid loss by ejection. At 1200 mPa s, the viscous friction dominates and the mass ratio k_m becomes independent of the gas supply rate (Figure 10c). Such high experimental liquid viscosities are, however, out of the scaled range for comparison with basaltic volcanic conduits (see section 5.3.). The actual ratio k_m of a basaltic eruption in the annular flow regime will depend on the effective liquid friction, i.e., on liquid viscosity and length of the conduit.

Series 2 experiments, in which admixing of small bubbles into the liquid was allowed, produced significant differences in the eruptive behavior. Such mixing dampens turbulence, and gas and liquid mass fluxes become linearly coupled (Figure 11). The increase in M_l with M_g decreases as liquid viscosity increases, and there is little change in M_l over the range of M_g at viscosities greater than 800 mPa s. The erupted mass ratio k_m in the annular flow regime is about 2-3 times lower than in comparable series 1 experiments without mixing. Mixing with gas bubbles increases the effective viscosity [*Prandtl et al.*, 1990] and friction at the conduit wall, which reduces the liquid output (lower value of k_m). Increasing and then decreasing the gas mass flux produces a hysteresis in the variation of M_l with M_g (Figure 12) which is probably caused by a continuous increase in viscosity with mixing time, thus reducing the liquid transport rate. Eruption duration thus has an influence on the mass balance of erupted gas and liquid.

4. Flow in a Rough-Walled Conduit

Natural volcanic conduits are not smooth cylindrical tubes of constant diameter as assumed in modeling and used in experiments but are rather characterized by lateral and vertical changes in diameter and axis location resulting from complex crack propagation through the multiple layers of a volcanic

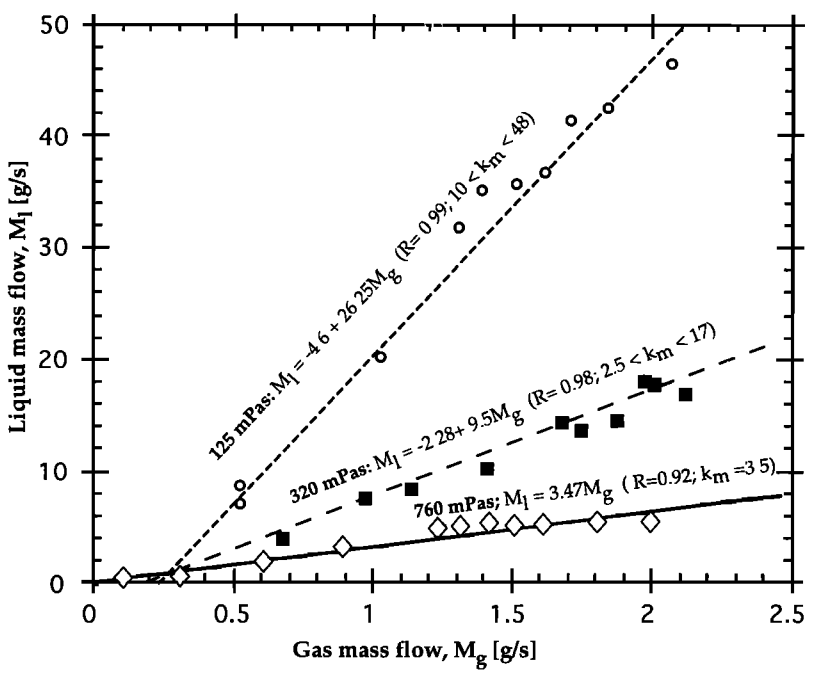

Figure 11. Results of series 2 experiments with continuous gas supply, allowing for mixing of bubbles into liquid. Liquid flux M_l varies linearly with gas flux M_g, and the slope decreases toward higher liquid viscosities.

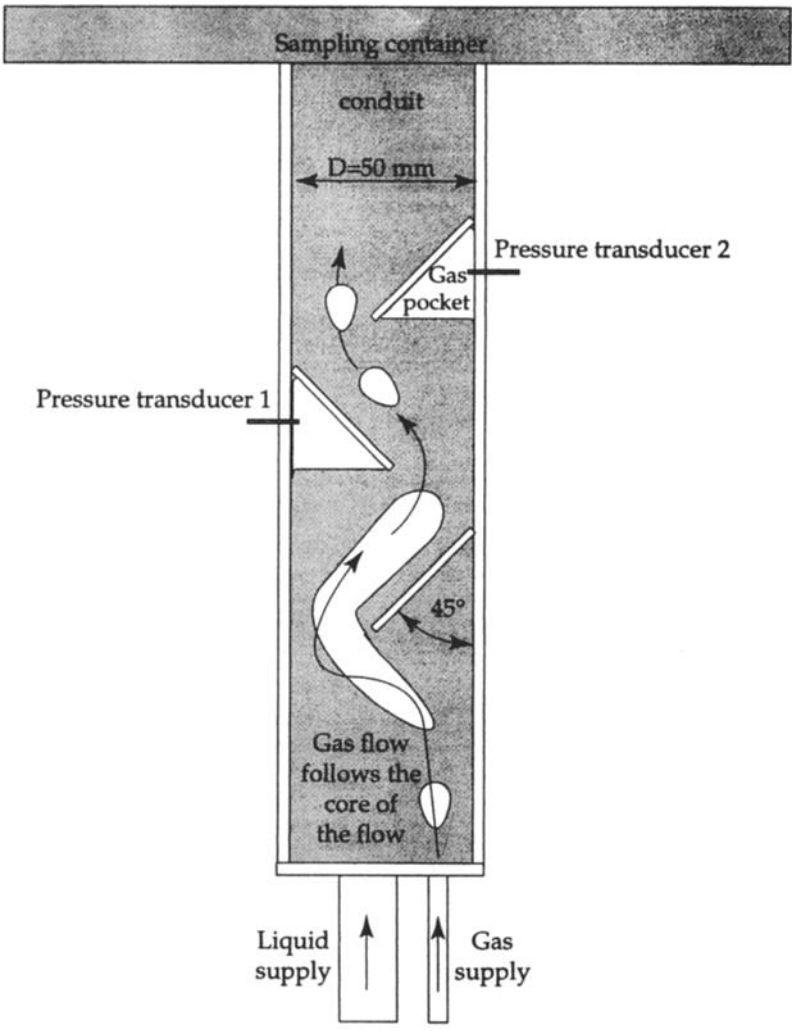

Figure 12. Experimental setup to investigate gas slug propagation through a partially blocked conduit. Pressure transducers mounted inside trapped gas pockets record their oscillation stimulated by the passing liquid.

edifice [e.g. *Ryan et al.,* 1981]. We used a perspex tube with built-in obstacles (Figure 12) to experimentally investigate the propagation of slug bubbles through a partially blocked conduit. Pressure sensors mounted below obstacles where gas could be trapped allowed us to record oscillation of the gas pockets stimulated by the passing liquid.

A first series of experiments used the partially blocked conduit filled with liquid of 850 mPa s viscosity connected to a large liquid reservoir. Gas injection began in the slug flow regime and was then driven into the annular flow regime. Gas pockets formed below the obstacles in the conduit, but when these were filled, the core flow of liquid and gas slugs moved around the obstacles (Figure 13). Gas slugs then deformed but remained intact during passage through the conduit, and no significant deviations in slug ascent velocity compared to a smooth conduit could be observed.

In a second set of experiments, gas was initially injected into the conduit wall pockets. Gas-free liquid was then pumped through the conduit, and the signals of two pressure transducers placed inside the gas pockets were recorded at a sampling rate of 11,025 Hz to detect the resonance frequencies. These pressure signals did not rise significantly above the noise level in all experiments. Furthermore, the signals produced by gas pocket oscillation were at least 3 orders of magnitude less powerful than those produced in the first experiments discussed above. There, strong pressure fluctuations were caused by rapid formation, coalescence, and expansion of slug bubbles and by turbulent mixing of liquid and gas. We conclude that these processes are the dominant sources of volcanic tremor, rather than the much less powerful oscillation of trapped gas pockets.

5. Eruption Phenomena

Each of the flow regimes in the experimental conduit produces a different style of eruption.

Single slug ascent can only develop from single, sudden incidents of limited-volume gas release which, in the volcanic environment, may occur, e.g., by local ground-water vaporization at the conduit wall or release of trapped gas pockets by volcanic shocks. Single slugs rise and burst at the surface causing short eruption pulses separated by irregular time intervals. We refer to this type of activity as sporadically pulsating lava fountains. The collapse of slug bubbles at the surface in our experiments was recorded on 16 mm high speed film with up to 2000 frames per second. The pictures (Figure 13) clearly show a rather quiet process, involving little fragmentation, where slug collapse took place at the

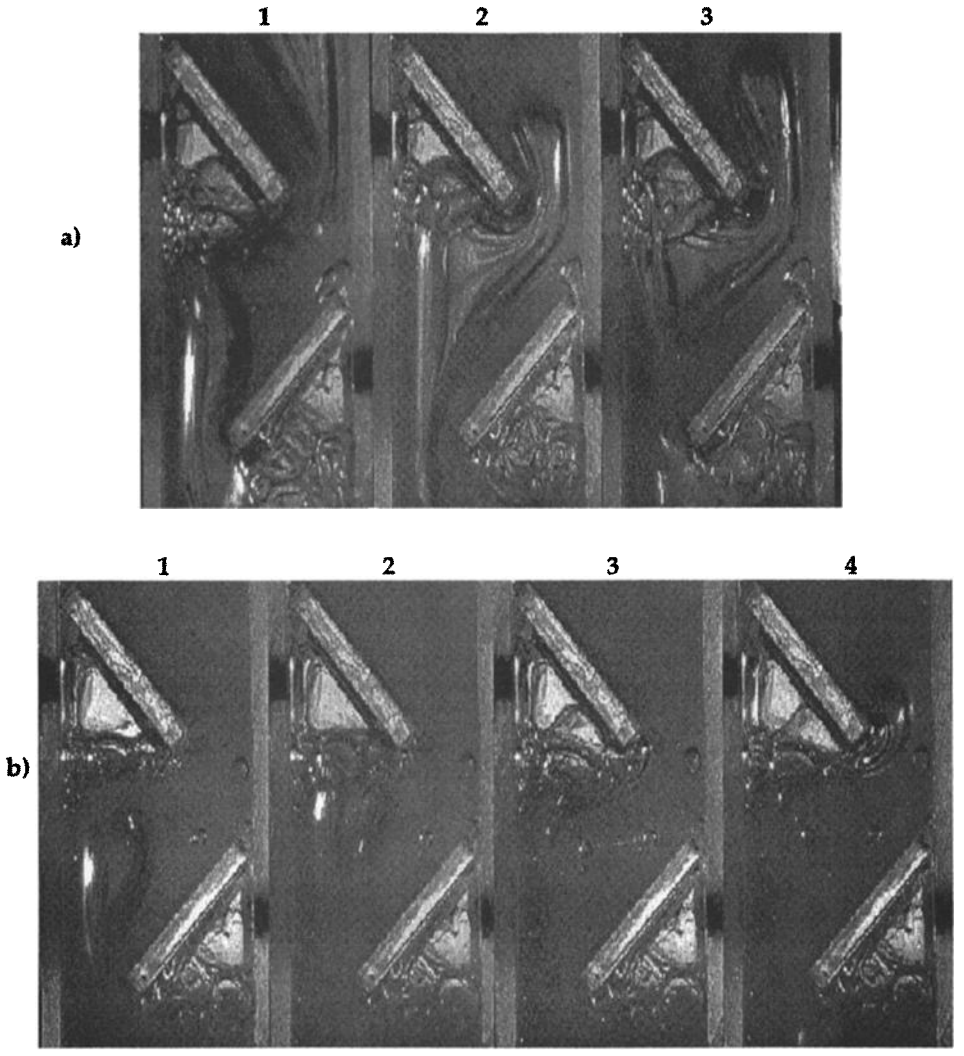

Figure 13. (a) Pictures taken at $\Delta t = 0.1$-s intervals from an experiment with the setup in Figure 12 showing the core of the slug flow moving around the obstacles which are already filled with trapped gas. (b) Sequence of pictures in the same setup showing bursting of bubbles into trapped gas pockets during coalescence.

liquid level inside the conduit. When the liquid level was in the reservoir atop the conduit (Figure 14) as in a lava-filled crater, however, bubble bursting and liquid ejection were more vigorous and resembled strombolian explosions. Because single slug ascent produces little mixing of gas and liquid, and thus does not significantly expand the liquid by foam formation, a slug formed by a quick pulse of gas injection had to be sufficiently long to push out any of the overlying liquid before disruption (Figure 15).

The periodicity of slug flow causes eruptions to occur at regular time intervals; we call this type of activity a periodically pulsating lava fountain.. However, whether or not liquid is exhausted from the conduit during slug flow depends on the depth of the static liquid level below the conduit exit before gas injection, the liquid viscosity, and the duration of gas supply. In our experiments using water (1 mPa s), the conduit had to be filled to the exit level to have measurable amounts of liquid ejected. At a viscosity of 100 mPa s, gas bubbles mixed into the liquid could escape only slowly and thus expanded the liquid column until the mixture reached the conduit exit from where it mainly flowed out effusively. As with single slugs, the mode of bubble disruption in the slug flow regime depends on whether it occurs inside the conduit or at the free surface.

Supplied slugs rise much faster through the volcanic conduit than single slugs and effectively push the overlying liquid effusively out of the conduit. When the slug cap bursts at the surface, the supplied slug breaks down into annular flow.

Annular flow thus can result from either a gradual increase in gas flux out of the slug-flow regime or from the collapse of a supplied slug. Annular flow always creates a fountain-like eruption with strong pulsations of higher frequency, reflecting the turbulence frequency of the conduit flow. Fragmentation of liquid is more efficient than in the slug flow regime, generating more and finer droplets. We refer to this style of eruption as a quasi-steady lava fountain. Experimental eruptions driven by annular flow with higher-viscosity liquids suffered waning liquid eruption rates in response to the friction-limited liquid supply (see section 3.2.3.), eventually resulting in ejection of gas only from the conduit. Our experiments suggest that when a quasi-steady fountain is preceded by Strombolian-type explosions, gas release at depth

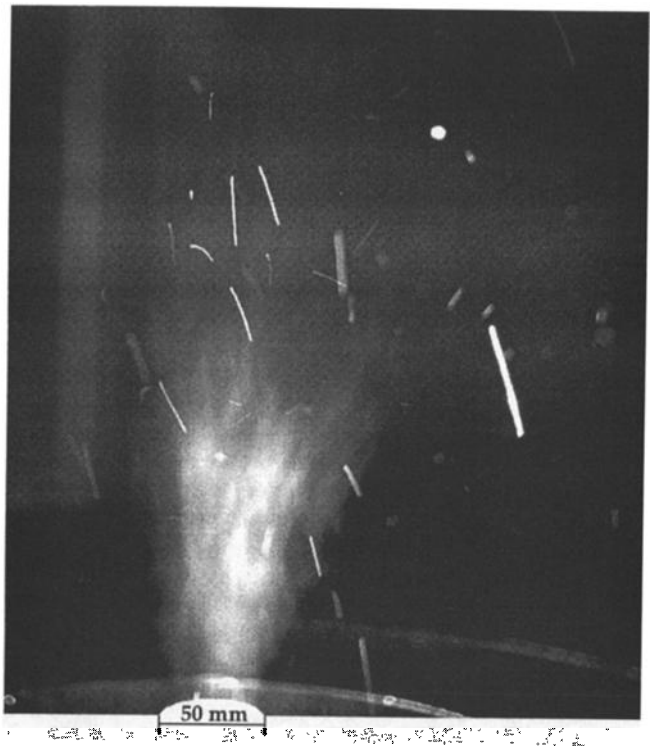

Figure 14. Photograph of a narrow fountain of strongly fragmented liquid erupted from the conduit during slug-annular flow. Liquid viscosity is $\mu = 125$ mPas and gas flux is $M_g = 0.8$ g/s.

was more gradual, whereas when it is preceded by lava effusion, gas was released rather catastrophically to form a supplied slug.

Our experiments provide no a priori characteristic to relate the eruption style to a certain source mechanism (process of gas release or generation) of the separated two-phase flow in the conduit. Dedicated experiments would be needed to identify distinguishing features, such as perhaps differences in the grain size distributions resulting from the different fragmentation mechanisms.

6. Conclusions

Our experimental study complements earlier analyses of homogeneous two-phase flow in basaltic volcanic conduits [*Wilson and Head*, 1981] by considering separated two-phase flow phenomena. Scaling of the experiments allows to apply our results to basaltic eruptions when natural complexities at a given volcano are adequately considered.

Single gas slugs can form in a volcanic conduit by sudden release or generation (e.g., by water vaporization) of a limited gas volume. The ascent velocity of single gas slugs then lies in the transitional regime at $0.1 < Fr^{0.5} < 0.345$. Ascent velocity is independent of decompressional slug growth during ascent but depends on liquid viscosity and weakly on the gas mass contained in a slug. The static magma level in the conduit has to reach the vent exit to produce significant Strombolian-type eruptions from single slug ascent. A steady gas release into the conduit at moderate rates breaks up into the slug flow regime, where liquid trapped between periodic gas slugs is carried upward and ejected as the bubbles burst at the conduit exit. Eruptions due to single-slug ascent occur irregularly in time, in contrast to rhythmical Strombolian-like eruptions that are due to slug flow. We therefore distinguish between sporadically pulsating lava fountains and periodically pulsating lava fountains. Backflow of liquid along the margins of gas slugs drives convection in the conduit. Liquid mixed with small bubbles, generated either in the turbulent wake of large slugs or during slug disruption at the surface, is thereby transferred into deeper regions of the conduit. Such processes may significantly modify bubble size distributions in the resulting volcanic rocks.

A supplied slug forms when a large volume of gas (greater than the conduit volume) is suddenly released into the conduit and remains connected to, and fed from, its gas reservoir throughout its ascent. Supplied slugs reach much higher velocities ($Fr^{0.5} = 0.15$-1.6 in the experiments) than unsupplied slugs. No backflow of liquid takes place, and overlying magma is driven effusively out of the conduit until the slug cap bursts at the surface and the supplied slug collapses to a highly turbulent two-phase flow in the conduit.

Turbulent annular flow generates quasi-steady lava fountains in which the mass ratio of liquid to gas is lower than in the slug flow and is controlled by the transport capacity of the gas stream. The mass ratio can decrease with time even at constant gas flux when the friction-controlled supply rate of liquid cannot keep pace with the eruption rate of liquid. Annular flow can form either by increasing the gas supply rate above the range for slug flow, or by collapse of supplied slugs. In both cases, the transition to annular flow involves a change from the hydrostatic to the much lower dynamic pressure gradient, reducing pressure in the reservoir and promoting further degassing of the magma which may maintain fountaining activity until the gas reservoir is exhausted.

In general, the erupted mass ratio of magma to gas depends on the rheology of the magma, the flow regime in the conduit, viscous friction in the plumbing system, and the mixing time of magma and gas during ascent and eruption. Our results are not apparently sensitive to conduit shape and roughness.

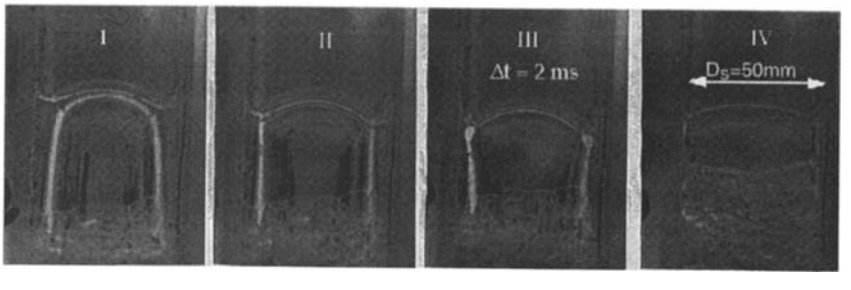

Figure 15. Four frames at $\Delta t = 2$ ms time intervals from 16-mm high-speed film recording. The collapse of a gas slug inside the conduit can be seen as a quiet process without oscillation or significant fragmentation.

Slugs remained stable without coalescence and significant velocity change during ascent in a partially blocked conduit. Bubble bursts during coalescence with gas pockets trapped in the corners of the blocked conduit appear to be a prominent source of volcanic tremor because they produced at least 3 orders of magnitude more powerful pressure signals than gas pocket oscillation induced by passing liquid.

Notation

A	cross-section area.
C	bubble concentration.
D	conduit diameter.
D´	corresponding tube diameter.
H	height of the magma chamber.
J	flux.
K	Karman´s constant (K = 0.4).
L	length.
M	mass flow.
N	dimensionless parameter relating film thickness and ascent velocity of slugs.
Q	bulk volume flux.
R	specific gas constant [J/Kg/K].
S	spring constant of a gas slug.
T	temperature.
T	temperature difference.
Tu	turbulence.
U	velocity.
V	volume.
c_r	flow restistance.
d_{sl}	slug diameter.
g	gravity acceleration.
k_m	mass ratio between magma and gas.
m	mass.
p	pressure.
t	time.
z	distance from the surface.
z_c	length of slug cap.
χ	dimensionless slug cap length.
δ	film thickness between slug and conduit wall.
λ	friction coefficient.
θ	damping factor.
ρ	liquid density.
σ	surface tension.
ξ	dimensionless film thickness.
μ	liquid viscosity.

Indices

an	annular flow.
2p	two phases.
g	gas.
l	liquid.
m	magma.
sf	slug flow regime.
sl	slug.

Acknowledgments. This work was funded by the Deutsche Forschungsgemeinschaft (DFG) through grants Fr947/3-1 and Fr947/3-2 to A. Freundt. We wish to thank K. Cashman, L. Wilson, and A. Woods for their comments on this paper.

References

Alibidirov, M., and D.B. Dingwell, Magma fragmentation by rapid decompression, *Nature, 380*, 146-148, 1996.

Brown, R., The mechanics of large gas bubbles in tubes, *Can. J. Chem. Eng.*, 43, 217-230, 1965.

Campos, J., and J. Guedes de Carvalho, An experimental study of the wake of gas slugs rising in liquids, *J. Fluid. Mech., 196*, 27-37, 1988.

Clift, R., *Bubbles, Drops and Particles*, 465 pp., Academic, San Diego, Calif. 1978.

Freundt, A., and R. Seyfried, Experiments on gas slug ascent, paper presented at IUGG Meeting, Boulder, Colo. 1995.

Gardner, J.E., R.M.E. Thomas, C. Jaupart, and S.R. Tait, Fragmentation of magma during plinian volcanic eruptions, *Bull. Volcanol., 48*, 144-162, 1996.

Herd, R., and H. Pinkerton, Bubble coalescence in basaltic lava: Its impact on the evolution of bubble populations, *J. Volcanol. Geotherm. Res., 75*, 137-157, 1997.

Jaupart, C., and S. Vergniolle, The generation and collapse of a foam layer at the roof of a basaltic magma chamber, *J. Fluid. Mech., 203*, 347-380, 1989.

Kieffer, S.W., Sound speed in liquid-gas mixtures: Water-air, water-steam, *J. Geophys. Res., 82*, 2895-2904, 1977.

Mader, H.M., Y. Zhang, J.C. Phillips, R.S.J. Sparks, B. Sturtevant, and E. Stolper, Experimental simulations of explosive degassing of magma, *Nature, 372*, 85-88, 1994.

Papale, P., Strain induced magma fragmentation in explosive eruptions, *Nature, 397*, 425-428, 1999.

Parfitt, E.A., and L. Wilson, Explosive volcanic eruptions, IX, The transition between hawaiian-style lava fountaining and Strombolian explosive activity, *Geophys. J. Int., 11*, 226-232, 1995.

Peebles, N., and H.J. Garber, Studies of the motion of gas bubbles in liquids, *Chem. Eng. Progr., 49*, 88-97, 1953.

Prandtl, L., K. Oswatitsch, and K. Wieghard, *Führer durch die Strömungslehre*, 563 pp., Vieweg, Brunswick, Germany, 1990.

Proussevitch, A.A., D.L. Sahagian, and Kutolin, The stability of foams in silicatic melts, *J. Volcanol. Geotherm. Res., 59*, 161-178, 1993a.

Proussevitch, A., D.L. Sahagian, and A.T. Anderson, Dynamics of diffusive bubble growth in magmas: Isothermal case, *J. Geophys. Res*, *98*, 22,283-22,307, 1993b

Ryan, M.P., R.Y. Koyanagi, and R.S. Fiske, Modeling the 3-dimensional structure of macroscopic magma transport systems: application to Kilauea volcano, Hawaii, *J. Geophys. Res*, *86*, 7111-7129, 1981.

Simkin, T., and L. Siebert, *Volcanoes of the World*, Geosience, Tucson, Ariz., 1994.

Sparks, R.S.J., The dynamics of bubble formation and growth in magmas: A review and analysis, *J. Volcanol Geotherm Res., 3*, 137-186, 1978.

Stein, D., and F. Spera, Rheology and microstructure of magmatic emulsions: theory and experiment, *J. Volcanol. Geotherm. Res., 49*, 157-174, 1992.

Sugioka, I., and M. Bursik, Explosive fragmentation of erupting magma, *Nature, 373*, 689-692, 1995.

Vergniolle, S., and C. Jaupart, Separated two phase flow and basaltic eruptions, *J. Geophys. Res.* 91, 12,842-12,860, 1986.

Vergniolle, S., and C. Jaupart, Dynamics of degassing at Kilauea Volcano, Hawaii, *J. Geophys. Res., 95*, 2793-2809, 1990.

Wallis, G B., *One Dimensional Two-Phase-Flow*, 1408 pp., McGraw-Hill, New York, 1969.

White, E.T., and R.H. Beardmore, The velocity of rise of single cylindrical air bubbles through liquids contained in vertical tubes, *Chem. Eng. Sci., 17*, 351-361, 1962.

Wilson, L., and J.W. Head, Ascent and eruption of basaltic magma on the Earth and Moon, *J. Geophys Res., 86*, 2971-3001, 1981.

Wilson, L., and J.W. Head, Nature of local magma storage zones and geometry of conduit systems below basaltic eruption sites: Pu'u O'o Kilauea, East Rift Hawaii example, *J. Geophys. Res., 93*, 14,785-47,792, 1988.

Woods, A., and A. Cardoso, Triggering basaltic volcanic eruptions by bubble-melt separation, *Nature, 385*, 518-520, 1997.

Zhang, A., B. Sturtevant, and E.M. Stolper, Dynamics of gas-driven eruptions: Experimental simulations using CO_2-H_2O-polymer system, *J. Geophys. Res., 102*, 3077-3096, 1997

R. Seyfried and A. Freundt, GEOMAR Forschungszentrum, Wischhofstr. 1-3, D-24148 Kiel, Germany. (rseyfried@geomar.de)

Received May 10, 1999; revised November 17, 1999; accepted March 16, 2000.